Numerical Simulation of Highly Efficient Lead-free MAGeI3 Based Perovskite Solar Cell for Various ETL and HTL Layers

Farjana Akter Jhuma
Interdisciplinary Graduate School of Engineering Sciences, Faculty of Engineering Sciences, Kyushu University

Mohammad Junaebur Rashid
Department of Electrical and Electronic Engineering, Faculty of Engineering and Technology, University of Dhaka

Islam, Sharnali
Department of Electrical and Electronic Engineering, Faculty of Engineering and Technology, University of Dhaka

https://doi.org/10.5109/5909089

出版情報：Proceedings of International Exchange and Innovation Conference on Engineering & Sciences (IEICES). 8, pp.183-188, 2022-10-20. Interdisciplinary Graduate School of Engineering Sciences, Kyushu University
バージョン：

Proceedings of the 8th International Exchange and Innovation Conference on Engineering & Sciences (IEICES 2022)

Numerical Simulation of Highly Efficient Lead-free $MAGeI_3$ Based Perovskite Solar Cell for Various ETL and HTL Layers

Farjana Akter Jhuma[1*], Mohammad Junaebur Rashid[2], Sharnali Islam[2]
[1]Interdisciplinary Graduate School of Engineering Sciences, Faculty of Engineering Sciences, Kyushu University, Japan
[2]Department of Electrical and Electronic Engineering, Faculty of Engineering and Technology, University of Dhaka, Bangladesh
*Corresponding author email: farjana.jhuma.13@gmail.com

Abstract: *The eco-friendly and highly stable lead-free $MAGeI_3$ perovskite solar cell has proved itself as a potential candidate for conventional lead-based perovskite solar cells with high efficiency. In this paper, numerical simulation has been performed over $MAGeI_3$ solar cell with three different Electron Transport Layer (ETL) and Hole Transport Layer (HTL) materials to obtain the best combination of ETL/perovskite/HTL layers using the solar cell simulation tool SCAPS-1D. The best performance has been found for the ITO/ZnO/$MAGeI_3$/NiO_x structure with an efficiency of 21.19% (V_{oc} of 1.89 V, J_{sc} of 16.11 mA/cm^2, and FF of 69.57%) due to the higher bandgap and better carrier mobility of these two ETL and HTL materials. The thickness optimization indicated that a thickness below 1000 nm is suitable for better performance which also leads to a good indication of making a lightweight solar cell. This study indicates that the use of low-cost and environment-friendly ZnO and NiO_x with non-toxic $MAGeI_3$ perovskite has the potential to obtain a high-efficiency eco-friendly solar cell.*

Keywords: $MAGeI_3$ perovskite solar cell; Electron Transport Layer (ETL); Hole Transport Layer (HTL); SCAPS-1D.

1. INTRODUCTION

The global demand for renewable and green energy for power generation in the last few decades has developed a vast field of research for new inventions with low-cost and highly efficient photovoltaic devices. The perovskite-based photovoltaic cells have also gotten the attention of researchers due to their favorable inherent characteristics like tunable direct bandgap, higher absorption coefficient, low exciton binding energy, and higher carrier mobility as well as easier and cost-effective fabrication process [1-4]. The first perovskite solar cell was introduced by Kojima et.al. in 2009 using Iodine (I^-) as the halide material which only had a conversion efficiency of 3.81% [5], But after a decade it has advanced to 25.8% by a group of researchers who introduced an interlayer between the perovskite $FAPbI_3$ and charge transporting layer to reduce the defects [6]. Despite offering higher efficiency, the Lead (Pb)-based perovskite is still facing issues in the case of using the device commercially due to the toxicity of Pb leading to some technical and environmental issues [7] So, it is necessary to find alternatives to Pb to make a highly efficient environment-friendly solar cell. Non-toxic metals such as tin (Sn), bismuth (Bi), and germanium (Ge) can work as alternatives [7-9]. Though having the possibility to be an alternative to Pb ion, both Sn^{2+} and Bi^{3+} undergo instability at the time of inclusion with the other ions of perovskite material [10]. Ge doesn't face this kind of problem which leads it to be a good candidate for the replacement of lead from the perovskite material. Ge-based absorber layer (Methylammonium Germanium tri-iodide, $MAGeI_3$) can provide more stability than the lead-based counterpart as the absorber layer (Methylammonium Lead tri-Iodide, $MAPbI_3$) in a perovskite solar cell due to the use of less degradable Ge instead of Pb [11]. Ge can provide higher stability at higher temperatures up to 150 ^{0}C, making it more suitable for the fabrication of the solar cell [11]. The excellent electron and hole transport nature, and suitable absorption in the range of 350 nm-650 nm due to the narrower bandgap of $MAGeI_3$ have made it a potential competitor of $MAPbI_3$ to make a highly efficient eco-friendly solar cell [12]. For this reason, $MAGeI_3$ has been chosen in this paper as the active layer material of the solar cell.

For obtaining a highly efficient perovskite solar cell, one of the major requirements is to optimize the charge transport layers (CTLs). The efficiency of the cell highly depends on the carrier mobilities of the CTL and its band alignment with the perovskite absorber. Efficient transmission of both electrons and holes throughout the device is crucial for a high-performance solar cell which can be obtained by making a good combination of ETL (Electron Transport Layer) and HTL (Hole Transport Layer) material selection. Many researchers have tried to optimize the $MAGeI_3$ solar cell's performance with different ETL and HTL combinations [13-14]. The most used ETL material is TiO_2, but it suffers from lower - carrier mobility and less stability under UV illumination [15]. Other materials like ZnO, IGZO, PCBM, etc. have also been used as the ETL material [13]. For the case of HTL material, the use of D-PBTTT-14 in $MAGeI_3$ showed an efficiency of greater than 21% [14]. Other materials like P3HT, CuSCN, Spiro-OMeTAD, Cu_2O, etc. have also been adopted as the HTL material of $MAGeI_3$ perovskite solar cell [13-14].

Taking the above issues in mind, in this work, we tried to investigate the effect of different ETLs and HTLs on the performance of $MAGeI_3$ solar cells using the solar cell simulation software SCAPS-1D (Solar Cell Capacitance Simulator). We used three different materials ZnO, WO_3, and SnO_2 as ETL while using NiO_x, CuI, and PEDOT: PSS as the HTL and tried to optimize the perovskite absorber layers' thickness for the best combination of ETL and HTL. The solar cell parameters open-circuit voltage (V_{oc}), short circuit current density (J_{sc}), fill factor (FF) and efficiency (η) has been calculated for optimizing the best-performing solar cell.

2. NUMERICAL MODELLING AND DEVICE STRUCTURE

The device structure used for the numerical study of the $MAGeI_3$ perovskite solar cell in this paper is represented in Fig. 1. The structure consisted of a hole transport layer just above the glass substrate at the very bottom and is used for blocking the electrons and transporting the holes over a glass substrate that is followed by the $MAGeI_3$ perovskite layer where most of the photons are absorbed. The next layer to the absorber is the electron transport layer for transporting the electron and blocking the holes in the electrodes. The structure is finally completed by a transparent conducting oxide layer. The light illuminates the cell through the ITO layer under the AM1.5 solar spectrum with an incident power density of $100W/m^2$. The layer parameters for all the layers used in the simulations have been summarized in Table 1 and Table 2 which are taken from different literature [13, 16-19].

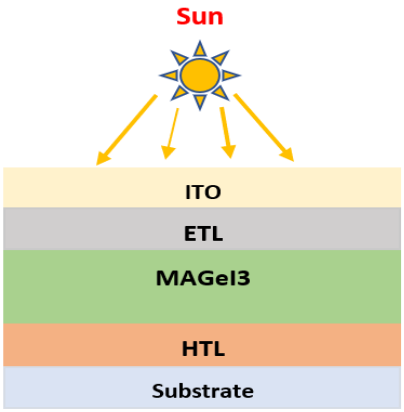

Fig. 1: The schematic of the structure of the $MAGeI_3$ solar cell

Table 1: Layer properties of different ETL & $MAGeI_3$

Parameters	ZnO	WO_3	SnO_2	$MAGeI_3$
E_g (eV)	3.3	2.92	3.5	1.9
χ (eV)	4.1	4.59	4	3.98
ε_r	9.0	5.76	9	10
N_c (cm^{-3})	4×10^{18}	1.96×10^{19}	2.2×10^{17}	1×10^{16}
N_v (cm^{-3})	1×10^{19}	1.96×10^{19}	2.2×10^{16}	1×10^{15}
μ_e (cm^2/V_s)	100	10	20	1.62×10^{1}
μ_h (cm^2/V_s)	25	10	10	1.01×10^{1}
N_D (cm^{-3})	1×10^{18}	3.68×10^{18}	1×10^{17}	1×10^{9}
N_A (cm^{-3})	0	0	0	1×10^{9}

To obtain the values of the solar cell performance parameters, numerical solar cell simulation software SCAPS-1D has been adopted in this study. SCAPS-1D was developed at the Department of Electronics and Information System (EIS) which supports the addition of up to 7 layers for a solar cell. This software can solve the basic semiconductor equation- the Poisson equation and the continuity equations for both electrons and holes in one-dimensional steady-state conditions and measure many properties like- short-circuit current density (J_{sc}), fill factor (FF), open-circuit voltage (V_{oc}), conversion efficiency (η), quantum efficiency (QE), spectral response, generation, and recombination profile, etc.

Table 2: Layer properties of different HTL

Parameters	NiOx	CuI	PEDOT:PSS
E_g (eV)	3.75	3.5	1.6
χ (eV)	2.10	2.1	3.4
ε_r	10.70	6.5	3
N_c (cm^{-3})	2.8×10^{19}	2.8×10^{19}	2.2×10^{18}
N_v (cm^{-3})	1.8×10^{19}	1×10^{19}	1.8×10^{19}
μ_e (cm^2/V_s)	12	1.7×10^{-4}	4.5×10^{-1}
μ_h (cm^2/V_s)	25	2×10^{-4}	9.9×10^{-5}
N_D (cm^{-3})	0	0	0
N_A (cm^{-3})	1×10^{15}	1×10^{18}	1×10^{16}

In this work, optimization of the thickness of the $MAGeI_3$ layer for different ETL and HTL layers have been tried to be done. During each simulation, the ETL and HTL layer thicknesses have been fixed at 50 nm while the ITO layer thickness has been maintained to be 60 nm. For the $MAGeI_3$ layer, the thickness has been changed from 300 nm to 1500 nm with a 300 nm step thickness for finding the best thickness where the cell performs the best. Au has been used as the back contact material throughout the simulation for the optimization of perovskite layer thickness.

3. RESULT AND DISCUSSION

3.1 Effect of perovskite thickness

Solar cell efficiency largely relies on the absorbance of the solar spectrum by the absorber layer which is influenced by the thickness variation of the layer. In this section, we have observed the effect of thickness variation on the performance parameters of solar cells i.e., open-circuit voltage (V_{oc}), short circuit current density (J_{sc}), fill factor (FF), and efficiency (η) for three different ETL material- ZnO, SnO_2 and WO_3 and also for three different HTL material- NiO_x, CuI, and PEDOT: PSS. In the case of observing the variation of different ETL, NiO_x has been used as the HTL material whereas in the time of HTL variation ZnO has been used as the ETL material.

3.1.1 Simulation with different ETL

Fig. 2 shows the variation of the solar cell parameters with increasing perovskite thickness for three different ETL layers- ZnO, SnO_2, and WO_3. In all graphs, the black line represents the changes for ZnO, the blue one stands for the changes due to SnO_2, and finally, the red one is used to show the variations for the WO_3 ETL layer. It is to be noted that, for V_{oc}, FF, and efficiency curves WO_3 shows lower performance than the other two materials. This is due to their bandgap phenomena. WO_3 has a bandgap of 2.92 eV which is lower than the other two ETL materials ZnO (3.3 eV) and SnO_2 (3.5 eV). The open-circuit voltage of a solar cell is given by:

$$V_{oc} = \frac{kT}{q} \ln\left(\frac{J_{ph}}{J_0} + 1\right) \quad (1)$$

Where kT/q defines the thermal voltage, J_{ph} and J_0 represent the light-induced current density and the diode saturation current density respectively. J_0 can be further obtained by the following equation:

$$J_0 = qn_i^2\left(\frac{D_N}{L_N N_A} + \frac{D_P}{L_P N_D}\right) \quad (2)$$

D_N and D_P in the above equation denote the diffusion constants for electron on the p-side and holes on the n-side of the junction correspondingly whereas, L_N and L_P stand for the electron and hole diffusion length on the p-side and n-side of the junction respectively. The net acceptor impurity concentration on the p-side and donor concentration on the n-side are denoted by N_A and N_D in the equation.

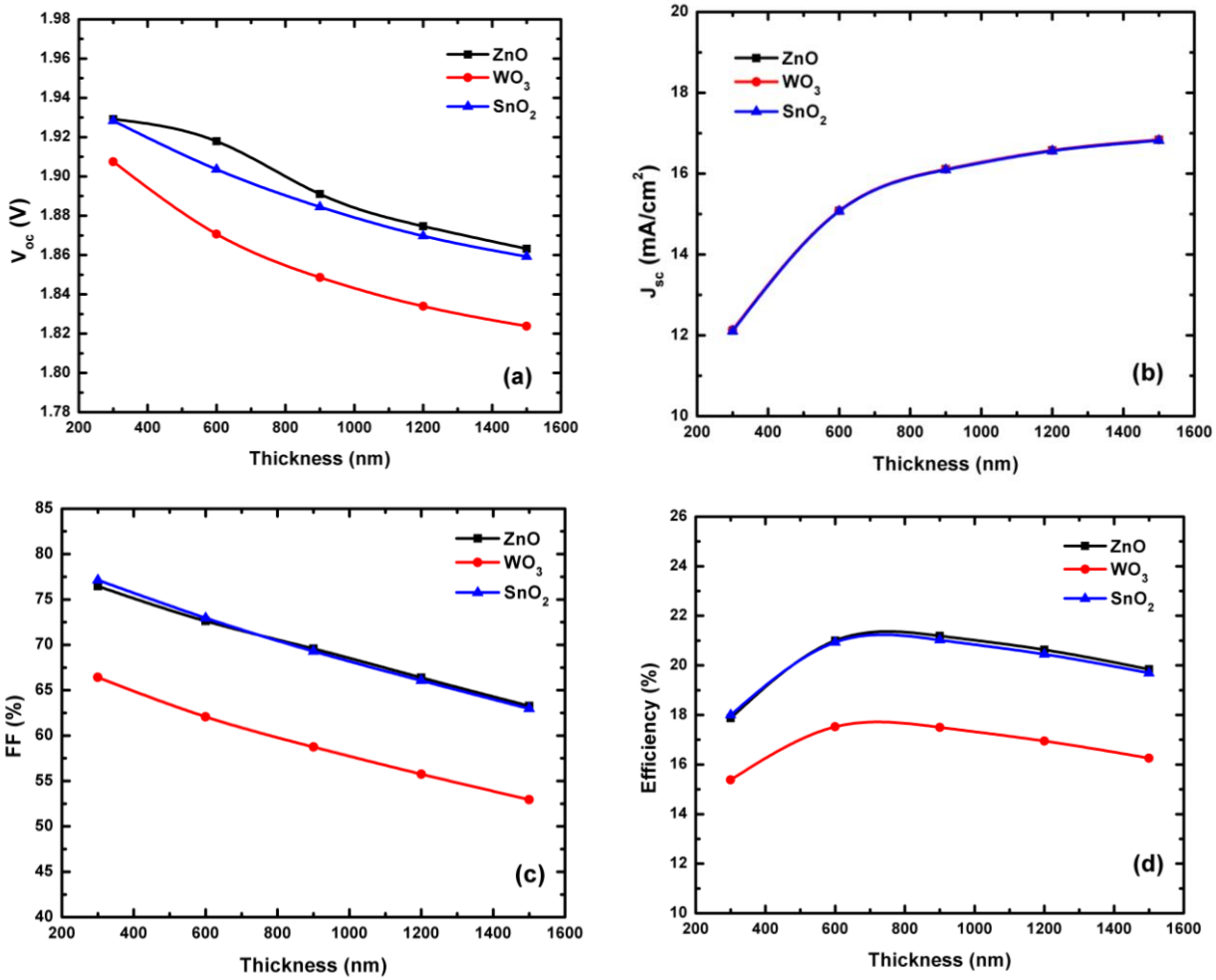

Fig. 2: Variation of (a) V_{oc}, (b) J_{sc}, (c) Fill Factor and (d) efficiency for perovskite thickness variation for different ETL

The square of the intrinsic carrier concentration, n_i, can be given by:

$$n_i^2 = N_C N_V \exp\left[-\frac{E_g}{kT}\right] \quad (3)$$

Where E_g is denoted as the bandgap of the material and N_c and N_v define the conduction band and valence band effective density of states of the charge carriers. From these above equations, it can be observed that V_{oc} is a function of the bandgap. With the increase in the bandgap, the diode saturation current density increases which in turn results in the reduction of V_{oc} [20]. For this reason, lower performance is found in the case of WO_3 which possesses a lower bandgap. This phenomenon contradicts ZnO and SnO_2. Though SnO_2 has a higher bandgap, it has lower V_{oc} than ZnO which is due to the higher mobility of ZnO [13].

Fig. 2(a) shows the variation of V_{oc} with the perovskite $MAGeI_3$ thickness. From the figure, it can be seen that the V_{oc} decreases with increasing perovskite thickness. As the thickness of the perovskite layer increases, the electron-hole recombination process increases which can increase the diode saturation current density, J_0 [21]. It is evident from equation (1) that an increase in J_0 will reduce the V_{oc} as they have an inversely proportional relation and so with the increase in thickness the V_{oc} value decrease. Next Fig. 2(b) shows the variation of J_{sc} with increasing perovskite thickness. As the perovskite layer becomes thicker with increasing thickness, the possibility to absorb more photons increases which in turn increases the open-circuit value of short circuit current density. Followingly, Fig. 2(c) shows the change of fill factor concerning thickness change which shows a similar kind of behavior of V_{oc}. Finally, Fig. 2(d) shows the effect of thickness variation on solar cell efficiency. At lower thickness (below 400 nm) the efficiency is lower due to the chance of electron-hole recombination before reaching the perovskite/ETL or perovskite/HTL interface. But with progress in the thickness of perovskite

more photons are absorbed which results in the generation of more electron-hole pairs. But after a certain thickness (for each ETL 900 nm) the efficiency starts to deteriorate again as the charge carriers cross their minority carrier diffusion length and the chance of electron-hole recombination increases [22]. The best efficiency has been found for ZnO/$MAGeI_3$ structure and it is 21.19 % with a V_{oc} of 1.89 V, J_{sc} of 16.11 mA/$cm^{2,}$ and FF of 69.57%. The best efficiencies for all 3 ETL materials are summarized in Table 3.

The J-V characteristics and external quantum efficiency (EQE) graphs of the simulated solar cell for different ETLs have been displayed in Fig. 3 which were obtained at the optimized thickness of the $MAGeI_3$ layer. The S-shaped J-V characteristics curve in Fig. 3(a) has been found due to the higher recombination of charge carriers at the thicker absorber layer. There is an almost identical shape for ZnO and SnO_2 whereas the curve for WO_3 indicates a lower performance because of its lower bandgap. The EQE curves for three ETL materials are identical shown in Fig. 3(b) which indicates zero contribution of them to the device carrier generation mechanism

Table 3: Variation for different ETL materials

ETL material	V_{oc} (V)	J_{sc} (mA/cm^2)	FF (%)	Efficiency (%)
ZnO	1.89	16.1075	69.57	21.19
WO_3	1.87	15.0838	62.08	17.52
SnO_2	1.88	16.0942	69.29	21.02

.

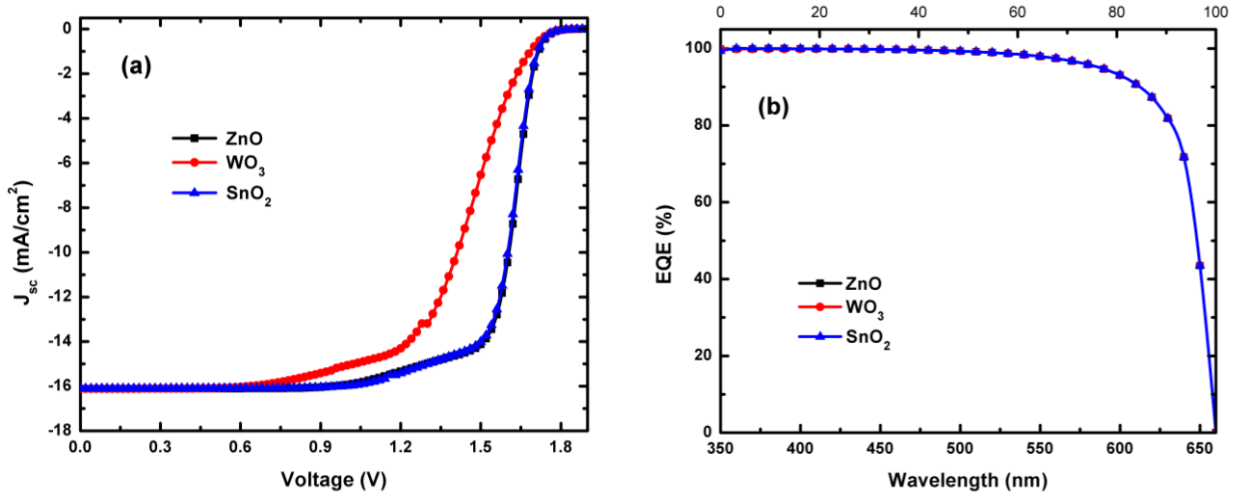

Fig. 3: (a) J-V curves and (b) EQE characteristics for different ETL in the $MAGeI_3$ solar cell.

3.1.2 Simulation with different HTL

Fig. 4 shows the solar cell parameter variation for different HTL layers- NiO_x, CuI, and PEDOT:PSS with the increase in perovskite layer thickness. In all graphs, black lines were used for NiO_x, red lines for CuI, and blue lines for PEDOT:PSS for indicating the changes. For the case of these three HTL materials, NiO_x has the highest bandgap (3.75 eV) than the other two materials and so it shows better performance which can be observed in Fig. 4. The reason behind this has been discussed in the previous section. Though CuI (2.98 eV) has a higher bandgap than PEDOT:PSS (2.2 eV), it shows lower performances in some cases due to its lower carrier mobility than PEDOT:PSS.

Fig. 4(a) shows the variation of V_{oc} for the increase in perovskite layer thickness. The V_{oc} value decreases almost linearly with the increase in perovskite layer thickness due to the increase of diode saturation current with increasing thickness [20]. Followingly, Fig. 4(b) shows the variation of J_{sc} with perovskite thickness where for all the cases value of Jsc increases with the increasing perovskite layer. But for the case of PEDOT:PSS the value is higher than the other two materials which may be higher absorption of photons due to the bandgap variation of the materials. Next, Fig. 4(c) shows the variation of the fill factor. For all three materials, FF shows a decreasing trend when the perovskite layer thickness increases. Finally, Fig. 4(d) shows the effect on solar cell efficiency. At lower thickness, the efficiency value is lower which then increases up to a certain thickness and after that starts to decrease with increasing thickness. The reason behind this phenomenon has been discussed in the previous section. Among the three structures, the best efficiency has been found for NiO_x/$MAGeI_3$ structure and the value is 21.19 % with a V_{oc} of 1.89 V, J_{sc} of 16.11 mA/$cm^{2,}$ and FF of 69.57%. The best efficiencies for all 3 HTL materials are concise in Table 4.

Table 4: Variation for different HTL materials

HTL material	V_{oc} (V)	J_{sc} (mA/cm^2)	FF (%)	Efficiency (%)
NiO_x	1.89	16.1075	69.57	21.19
CuI	1.88	16.1074	54.55	16.60
PEDOT:PSS	1.58	16.5862	65.44	17.21

Fig. 5 shows the J-V characteristics and EQE curves for a variety of HTL materials. S-shaped J-V curves for NiO_x and CuI have been displayed in Fig. 5(a) while for PEDOT:PSS, the value of J_{sc} concerning V just rises after 1.3 V. The EQE curves for the three HTLs have been displayed in Fig. 5(b) showing almost the same look. The EQE for CuI just shows a higher value from 600 nm to 650 nm rather than the two others for its lower mobility.

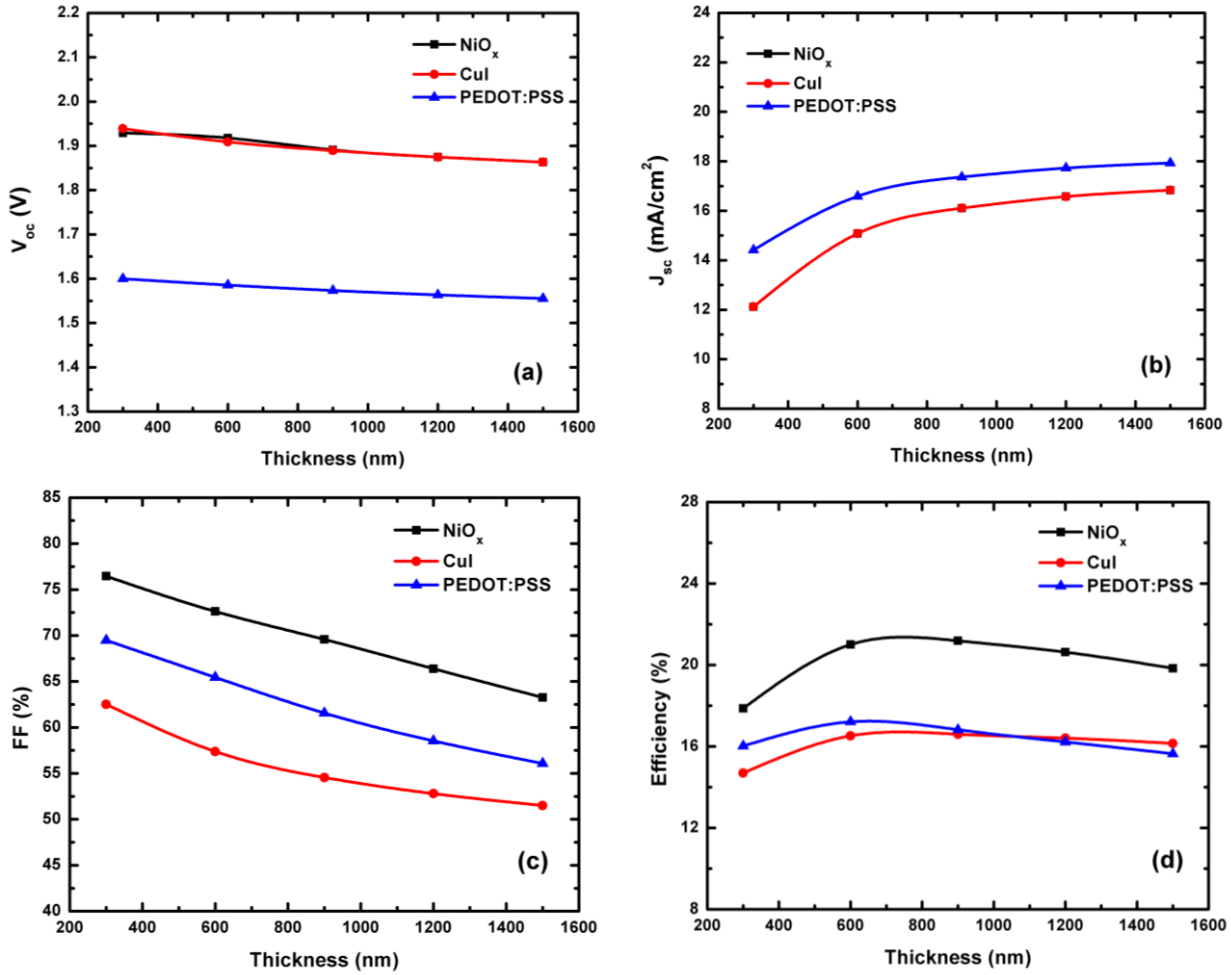

Fig. 4: Variation of (a) V_{oc}, (b) J_{sc}, (c) Fill Factor and (d) efficiency for perovskite thickness variation for different HTL

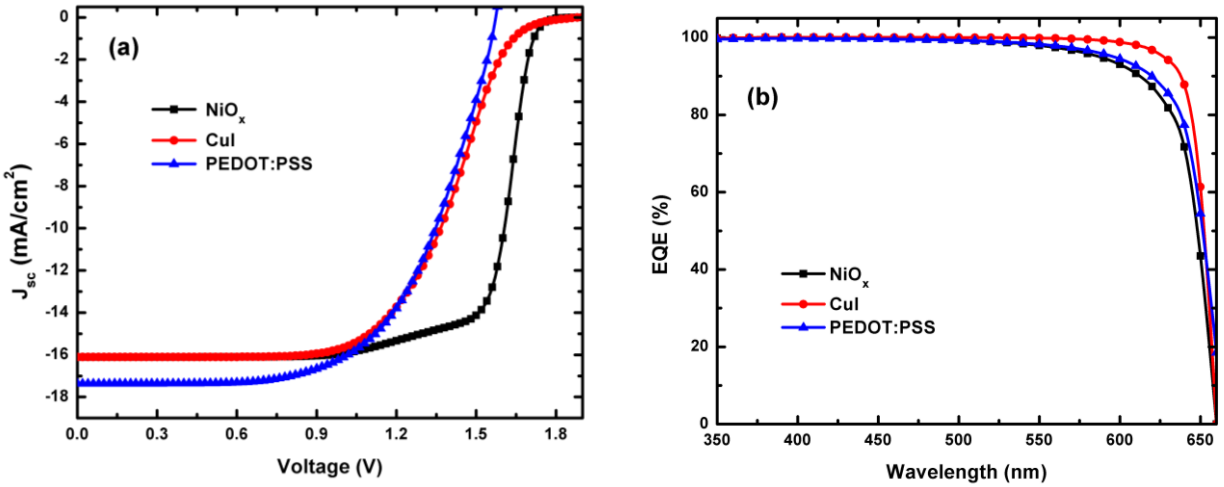

Fig. 5: (a) J-V curves and (b) EQE characteristics for different HTL in the $MAGeI_3$ solar cell.

4. CONCLUSION

In this paper, the performance analysis of $MAGeI_3$ solar cell with three different ETL and HTL layers has been done through numerical simulation using SCAPS-1D. From the thickness variation analysis of the perovskite layer, it has been found that the thickness of the perovskite layer should be kept between 600 nm-900 nm to obtain the best performance of the cell. Below this thickness range, there will be a limited number of photogenerated carriers to help to boost the efficiency and above the thickness range, the recombination process will be dominant to suppress the efficiency. The best performing solar cell has been found with the combination of ZnO ETL layer and NiO_x HTL layer with an efficiency of 21.19%. As both ZnO and NiO_x are environment-friendly and cost-effective materials, their combination with $MAGeI_3$ perovskite absorber can provide an eco-friendly low-cost solar cell with good efficiency.

REFERENCES

[1] J. H. Noh, S. H. Im, J. H. Heo, T. N. Mandal, S. Ll. Seok, Chemical Management for Colorful, Efficient, And Stable Inorganic–Organic Hybrid Nanostructured Solar Cells, Nano Lett. 13 (2013) 1764-1769

[2] J. Huang, Y. Yuan, Y. Shao, Y. Yan, Understanding the Physical Properties Of Hybrid Perovskites For Photovoltaic Applications, Nat. Rev. Mater. 2 (2017) 17042.

[3] W. Zhang, G. E. Eperon, H. J. Snaith, Metal halide perovskites for energy applications, Nat. Energy 1 (2016) 16048.

[4] Y. Zhao, K. Zhu, Organic–inorganic hybrid lead halide perovskites for optoelectronic and electronic applications, Chem. Soc. Rev. 45 (2016) 655-689.

[5] A. Kojima, K. Teshima, Y. Shirai, T. Miyasaka, Organometal Halide Perovskites as Visible-Light Sensitizers for Photovoltaic Cells, J. Am. Chem. Soc. 131 (2009), 6050-6051.

[6] H. Min, D. Y. Lee, J. Kim, G. Kim, K. S. Lee, J. Kim, M. J. Paik, Y. K. Kim, K. S. Kim, M. G. Kim, T. J. Shin, S. Il. Seok, Perovskite solar cells with atomically coherent interlayers on SnO_2 electrodes, Nature. 598 (2021) 444-450.

[7] F. Hao, C. C. Stoumpos, R. P. H. Chang, M. G. Kanatzidis, Anomalous Band Gap Behavior in Mixed Sn and Pb Perovskites Enables Broadening of Absorption Spectrum in Solar Cells, J. Am. Chem. Soc. 136 (2014) 8094-8099.

[8] W. Hu, X. He, Z. Fang, W. Lian, Y. Shang, X. Li, W. Zhou, M. Zhang, T. Chan, Y. Lu, L. Zhang, L. Ding, S. Yang, Bulk heterojunction gifts bismuth-based lead-free perovskite solar cells with record efficiency, Nano Energy. 68 (2020) 104362.

[9] Yu-Q. Zhao, B. Liu, Z. L. Yu, D. Cao, M. Q. Cai, Tuning Charge Carrier Types, Superior Mobility and Absorption in Lead-free Perovskite $CH_3NH_3GeI_3$: Theoretical Study, Electrochim. Acta. 247 (2017) 891-898.

[10] T. B. Song, T. Yokoyama, C.C. Stoumpos, J. Logsdon, D.H. Cao, M. R. Wasielewski, S. Aramaki, M. G. Kanatzidis, Importance of reducing vapor atmosphere in the fabrication of tin-based perovskite solar cells J. Am. Chem. Soc., 139 (2017), pp. 836-842

[11] Z. Yi, N. H. Ladi, X. Shai, H. Li, Y. Shen, M. Wang, Will organic–inorganic hybrid halide lead perovskites be eliminated from optoelectronic applications? Nanoscale Adv. 1 (2019) 1276-1289.

[12] P. Sun, Q. Li, L. Yang, Z. Li, Theoretical insights into a potential lead-free hybrid perovskite: substituting Pb^{2+} with Ge^{2+}, Nanoscale. 8 (2015) 1503-1512.

[13] S. Bhattari, T. S. Das, Optimization of carrier transport materials for the performance enhancement of the $MAGeI_3$ based perovskite solar cell, Sol. Energy. 217 (2021) 200-207.

[14] A. A. Kanoun, M. B. Kanoun, A. E. Merad, S. G. Said, Toward development of high-performance perovskite solar cells based on $CH_3NH_3GeI_3$ using computational approach, Sol. Energy. 182 (2019) 237-244.

[15] W. Hu, Z. Wen, X. Yu, P. Qian, W. Lian, X. Li, Y. Shang, X. Wu, T. Chen, Y. Lu, M. Wang, S. Yang, In situ surface fluorination of TiO_2 nanocrystals reinforces interface binding of perovskite layer for highly efficient solar cells with dramatically enhanced ultaviolate-light stability, Adv. Science. 8 (2021) 2004662.

[16] M. S. Rahman, S. Miah, M. S. W. Marma, M. Ibrahim, "Numerical Simulation of $CsSnI_3$-Based Perovskite Solar Cells: Influence of Doped-Ito Front Contact," 2020 IEEE Region 10 Conference (Tencon) (2020) 140-145, Doi: 10.1109/Tencon50793.2020.9293828.

[17] M. K. Otoufi, M. Ranjbar, A. Kermanpur, N. Taghavinia, M. Minbashi, M. Forouzandeh, F. Ebadi, Enhanced Performance of Planar Perovskite Solar Cells Using Tio_2/Sno_2 and Tio_2/Wo_3 Bilayer Structures: Roles of The Interfacial Layers, Sol. Energy. 208 (2020) 697-707.

[18] H. Alipour, A. Ghadimi, Optimization of Lead-Free Perovskite Solar Cells in Normal-Structure with Wo3 and Water-Free PEDOT;PSS Composite for Hole Transport Layer By Scaps-1D Simulation, Opt. Mat. 120 (2021) 111432.

[19] N. Touafek, R. Mahamdi, C. Dridi, Boosting the Performance of Planar Inverted Perovskite Solar Cells Employing Graphene Oxide as Htl, Dig. J. Nanomater. Bios. 16 (2021) 705-712.

[20] M.A. Green, Solar Cells: Operating Principles, Technologies and System Applications, Eaglewood Clifs, Prentice Hall, USA, 1982.

[21] F. Anwar, R. Mahbub, S. S. Sattar, S. M. Ullah, Effect of different HTM layers and electrical parameters on ZnO nanorod-based lead-free perovskite solar cell for high efficiency performance, Int. J. Photoenergy. 2017 (2017) 9846310.

[22] F. A. Jhuma, M. Z. Shaily, M. J. Rashid, Towards high efficiency CZTS solar cell through buffer layer optimization, Mater. Renew. Sustain Energy. 8 (2019) 1-7.